

Organic & Biomolecular Chemistry

Accepted Manuscript



This is an *Accepted Manuscript*, which has been through the Royal Society of Chemistry peer review process and has been accepted for publication.

Accepted Manuscripts are published online shortly after acceptance, before technical editing, formatting and proof reading. Using this free service, authors can make their results available to the community, in citable form, before we publish the edited article. We will replace this *Accepted Manuscript* with the edited and formatted *Advance Article* as soon as it is available.

You can find more information about *Accepted Manuscripts* in the [Information for Authors](#).

Please note that technical editing may introduce minor changes to the text and/or graphics, which may alter content. The journal's standard [Terms & Conditions](#) and the [Ethical guidelines](#) still apply. In no event shall the Royal Society of Chemistry be held responsible for any errors or omissions in this *Accepted Manuscript* or any consequences arising from the use of any information it contains.

Cite this: DOI: 10.1039/c0xx00000x

ARTICLE TYPE

www.rsc.org/xxxxxx

Synthesis and Antifungal Activity of 1,2,3-Triazole Phenylhydrazone Derivatives

Zhi-Cheng Dai^{a,b}, Yong-Fei Chen^{a,b}, Mao Zhang^c, Sheng-Kun Li^{a,b}, Ting-Ting Yang^{a,b}, Li Shen^c, Jian-Xin Wang^{a,b}, Shao-Song Qian^d, Hai-Liang Zhu^d, Yong-Hao Ye^{*a,b}

5

Received (in XXX, XXX) Xth XXXXXXXXX 20XX, Accepted Xth XXXXXXXXX 20XX

DOI: 10.1039/b000000x

A series of 1,2,3-triazole phenylhydrazone were designed and synthesized as antifungal agents. Their structures were determined based on ¹H-NMR spectroscopy, MS, elemental analysis and X-ray single-crystal diffraction. The antifungal activities were evaluated against four phytopathogenic fungi including *Rhizoctonia solani*, *Sclerotinia sclerotiorum*, *Fusarium graminearum* and *Phytophthora capsici*, by mycelium growth inhibition method *in vitro*. Compound **5p** exhibited significant anti-phytopathogenic activity, with the EC₅₀ values of 0.18, 2.28, 1.01, and 1.85 μg·mL⁻¹, respectively. *In vivo* test demonstrated that **5p** was effective in control of rice sheath blight, rape sclerotinia rot and fusarium head blight. 3D-QSAR model was built for a systematic SAR profile to explore more potent 1,2,3-triazole phenylhydrazone analogs as novel fungicides.

Introduction

Plant diseases such as rice sheath blight (RSB), rape sclerotinia rot (RSR) and fusarium head blight (FHB) caused by *Rhizoctonia solani*, *Sclerotinia sclerotiorum*, and *Fusarium graminearum*, respectively, bring severe crop yield reduction and result in dramatic economic losses in agriculture.¹ With the development of modern agricultural industry, many pesticides such as Carbendazim, Validamycin and Azoxystrobin, were developed and applied to control these diseases. However, the emergence of multiple drug-resistance revealed the urgent need for new fungicides.²

1,2,3-Triazoles have been attracting the interest of organic chemists for new drugs development owing to they are associated with a broad spectrum of biological activities, including antibacterial,² anti-tubercular,³ anti-HIV,⁴ alpha-glycosidase inhibitory⁵ and antifungal.⁶ Recently, the agrochemical potential of 1,2,3-triazoles has also aroused concern. Some of them have been proved to possess moderate anti-phytopathogenic bioactivities.^{7,8} Meanwhile, as its isomer, 1,2,4-triazoles have gained researcher's great attention in crop protection since 1970s.⁹ Some of 1,2,4-triazole derivatives, such as Triadimefon, Tebuconazole, Tropicconazole, have been widely used as agricultural fungicides.¹⁰

In order to explore the potential antifungal activity of 1,2,3-triazoles, a series of triazole derivatives were designed and synthesized via Click chemistry, with Huisgen 1,3-dipolar cycloaddition reaction as the key step.¹¹ The presence of Cu(I) dramatically accelerates the rate and makes the reaction highly regioselective, leading to only 1,4-disubstituted isomers.¹²

Substituted aromatic rings were combined to 1,2,3-triazoles systems as a scaffold. Based on the structure of Zinoconazole,¹³ the phenylhydrazone moiety, which has been proved to potentiate antifungal activities, was introduced to reinforce the bioactivity of 1,2,3-triazoles.¹⁴

The antifungal activities of the synthesized compounds were evaluated *in vitro* against four important phytopathogenic fungi. The *in vivo* efficacies of compound **5p** or **5w** against plant diseases caused by *R. solani*, *S. sclerotiorum*, *F. graminearum*, were also evaluated.

Results and discussion

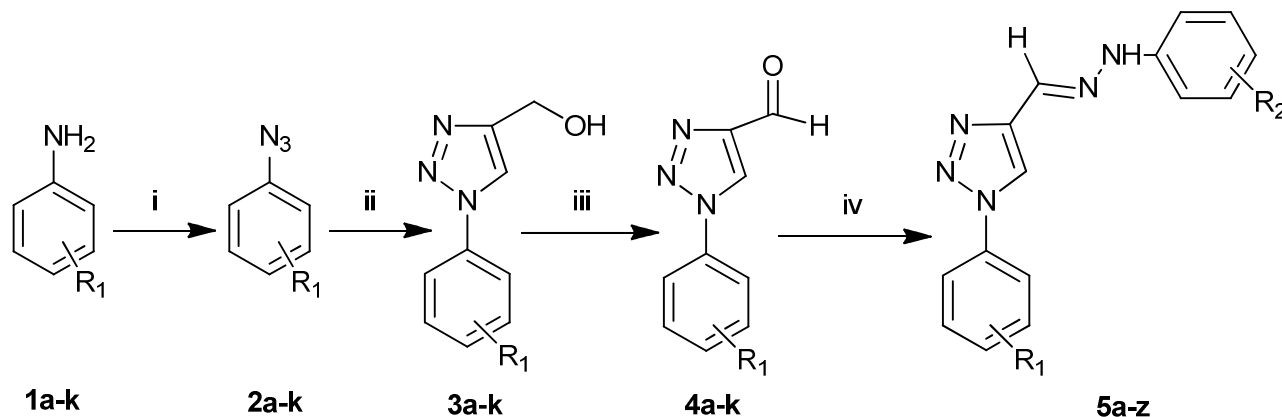
Chemistry

Synthesis of 1, 2, 3-triazole phenylhydrazone derivatives is outlined in Scheme 1. Compounds (**3a-k**) were prepared according to reported procedures.^{5,15} Different aromatic amines (**1a-k**) were diazotized by sodium nitrite to form diazonium salts, which were subsequently converted into azides (**2a-k**) with yields ranging from 60 % to 100 %. Then the azides were put directly in the next step without purification to prevent degradation. The synthesis of triazoles involved the 1,3-dipolar cycloaddition reaction between propargyl alcohol and aromatic azides (**2a-k**) which was catalyzed by Cu(I). Copper sulfate and sodium ascorbate guided the regioselectivity to obtain 1,4-disubstituted 1, 2, 3-triazoles. Reactions were performed at room temperature under photophobic condition to prevent aromatic azides from degradation. After purification in a flash column, 1,2,3-triazole alcohols (**3a-k**) were obtained as white or yellow crystals with

yields ranging from 40% to 80%.

1,2,3-Triazole alcohols (**3a-k**) were further oxidized to aldehydes (**4a-k**) using MnO_2 in ethyl acetate. The aldehydes were purified by filtration to remove the excess MnO_2 , compounds (**4a-k**) obtained as white or light-yellow crystals in yields ranging from 85% to 100%.¹⁶

Compounds (**4a-k**) were condensed to form the $-\text{C}=\text{N}-\text{NH}-$ bond with different substituted phenylhydrazine giving 1, 2, 3-triazole phenylhydrazone derivatives in yield of 68 – 85 %. $^1\text{H-NMR}$ spectroscopy, ESI-MS spectra and elemental analysis data of the target compounds were fully accordance with their assigned structures.



Scheme 1 Synthesis route of 1, 2, 3-triazole phenylhydrazone derivatives.

Reagents and conditions: (i) NaNO_2 , HCl 10%, 0-5°C; NaN_3 , 2-4 h, rt. (ii) propargyl alcohol, CuSO_4 , sodium ascorbate, $\text{H}_2\text{O}:t\text{-butanol}=1:1$, 24 h, rt; (iii) $\text{MnO}_2/\text{EtOAc}$, 1 h, rt; (iv) MeOH , substituted phenylhydrazine, 0.5 h, rt.

The crystal structure of compound **5l**

Among these compounds, crystal structure of compound **5l** was determined by X-ray diffraction analysis. Figure 1 gives a perspective view of **5l** with the atomic labelling system. The X-ray data have been deposited at the Cambridge Crystallographic Data Centre with the CCDC number 976935. The result demonstrates the $-\text{C}=\text{N}-\text{NH}-$ bond bears an (*E*)-configuration rather than (*Z*)-.

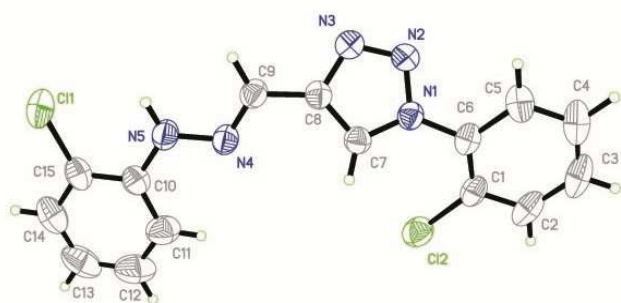


Fig.1 ORTEP view of compound **5l**

Antifungal activities *in vitro*

The concentration of initial antifungal activity screening *in vitro* was set as $25\mu\text{g}\cdot\text{mL}^{-1}$. If the inhibitory rate was greater than 50%, gradient concentrations of compounds would be treated to calculate their median effective concentration (EC_{50}) values.

Validamycin A, Carbendazim and Metalaxyl were co-assayed as the positive controls. The results suggested that most of the tested compounds showed considerable antifungal activities against *R. solani*, in which 7 compounds displayed potent activity with their EC_{50} values lower than $1\mu\text{g}\cdot\text{mL}^{-1}$. The EC_{50} value of the most potent compound **5p** ($0.18\mu\text{g}\cdot\text{mL}^{-1}$) is about 1 / 9 that of Carbendazim ($1.42\mu\text{g}\cdot\text{mL}^{-1}$). In addition, compound **5p** also significantly inhibited the mycelia growth of *S. sclerotiorum*, *F. graminearum* and *P. capsici*, with the EC_{50} values of 2.28, 1.01 and $1.85\mu\text{g}\cdot\text{mL}^{-1}$, respectively. It is worth noting that compound **5w** also showed good activities against four plant-pathogenic fungi, especially *F. graminearum* with an EC_{50} value of $0.61\mu\text{g}\cdot\text{mL}^{-1}$, comparable to the positive control Carbendazim ($0.50\mu\text{g}\cdot\text{mL}^{-1}$).

Structure and activity relationship (SAR) analysis indicated that halogen substituents of R_1 at *ortho* position, especially *o*-Cl (**5b**) and *o*-F (**5h**), always show advantage over those at *meta* or *para* positions. They were also effective against other three pathogens other than *R. solani*. If $\text{R}_1 = \text{ortho-Cl}$ (**5b**, **5l** – **5r**) or F (**5h**, **5s** – **5z**), it was more beneficial if R_2 was a *para* substituent. Among them, *para*-F analogues, such as **5p** and **5w**, displayed the most potent antifungal activities against four plant pathogens. This was consistent with the previous report that fluorine as a special atom can enhance the fungicidal activities when introduced into triazole derivatives.¹⁷

Table 1. The EC₅₀ values of compounds against four plant-pathogenic fungi *in vitro*^a

Compound	R ₁	R ₂	EC ₅₀ ±SD(μg·mL ⁻¹)			
			<i>R. solani</i>	<i>S. sclerotiorum</i>	<i>F. graminearum</i>	<i>P. capsici</i>
5a	H	H	3.01 ± 0.11	>25 ^b	>25	>25
5b	2-Cl	H	1.36 ± 0.55	4.80 ± 0.25	3.12 ± 0.24	7.39 ± 0.74
5c	3-Cl	H	75.32 ± 1.51	>25	>25	>25
5d	4-Cl	H	49.10 ± 1.70	>25	>25	>25
5e	2-Br	H	7.23 ± 0.32	>25	>25	>25
5f	3-Br	H	1.77 ± 0.55	>25	18.80 ± 0.23	20.30 ± 0.88
5g	4-Br	H	2.89 ± 0.43	>25	>25	>25
5h	2-F	H	1.61 ± 0.02	10.50 ± 0.21	7.37 ± 0.18	6.70 ± 0.19
5i	3-F	H	4.14 ± 0.05	>25	>25	>25
5j	4-F	H	1.91 ± 0.05	>25	21.43 ± 0.55	17.35 ± 0.34
5k	4-OMe	H	49.13 ± 0.75	>25	>25	>25
5l	2-Cl	2-Cl	3.08 ± 0.30	10.75 ± 0.35	>25	>25
5m	2-Cl	3-Cl	3.61 ± 0.09	>25	>25	>25
5n	2-Cl	4-Cl	0.65 ± 0.03	4.47 ± 0.37	1.95 ± 0.33	4.75 ± 0.38
5o	2-Cl	2-F	1.44 ± 0.03	9.93 ± 0.42	>25	13.29 ± 0.09
5p	2-Cl	4-F	0.18 ± 0.01	2.28 ± 0.01	1.01 ± 0.02	1.85 ± 0.02
5q	2-Cl	4-Br	0.80 ± 0.02	5.91 ± 0.03	1.74 ± 0.04	10.55 ± 0.05
5r	2-Cl	4-CF ₃	0.31 ± 0.01	12.84 ± 0.08	7.09 ± 0.03	>25
5s	2-F	2-Cl	30.51 ± 0.42	>25	>25	>25
5t	2-F	3-Cl	1.96 ± 0.12	>25	20.30 ± 0.33	>25
5u	2-F	4-Cl	0.34 ± 0.01	>25	>25	>25
5v	2-F	2-F	1.08 ± 0.02	>25	>25	>25
5w	2-F	4-F	0.63 ± 0.01	2.56 ± 0.04	0.61 ± 0.01	1.87 ± 0.02
5x	2-F	4-Br	0.80 ± 0.02	>25	>25	>25
5y	2-F	4-OMe	3.32 ± 0.11	3.78 ± 0.04	>25	>25
5z	2-F	4-Me	1.44 ± 0.02	3.43 ± 0.10	1.86 ± 0.08	10.54 ± 0.12
Validamycin A			5.07 ± 0.28	-	-	-
Carbendazim			1.42 ± 0.14	0.15 ± 0.03	0.50 ± 0.08	-
Metalaxyl			-	-	-	0.27 ± 0.18

^aValues are the mean ± SD of three replicates.^bInhibitory rate is below 50% at 25μg·mL⁻¹

3D-QSAR

In order to obtain a systematic SAR profile on 1,2,3-triazole analogs as antifungal agents and to explore the more potent inhibitors against *R. solani*, 3D-QSAR model was built and performed by built-in QSAR software of DS 3.5 (Discovery Studio 3.5, Accelrys, Co. Ltd). The training and test sets were divided by the random diverse molecules method of DS 3.5, in which the training set accounted for 80% of all the molecules while the test set was set to 20%.¹⁸ As listed in Table 2, the actual

pEC₅₀ values were converted from the obtained EC₅₀ values of *R. solani* inhibition. The predicted values and the corresponding residual values for the training set and test set molecules in 3D-QSAR model were also listed.

As shown in Figure 2A, the predicted values pEC₅₀ was associated with the experimental values with a correlation coefficient of 0.7930, suggesting that this model could provide a relatively accurate algorithm to predict the activity for 1,2,3-triazole derivatives against *R. solani*. A contour plot of the

electrostatic field region favorable (blue) or unfavorable (red) for antifungal activities was displayed in Figure 2B, while the energy grids corresponding to the favorable (green) or unfavorable (yellow) steric effects for the *R. solani* inhibition were displayed in Figure 2C. It was widely acceptable that a better inhibitor based on the 3D-QSAR model should have a strong Van der Waals attraction in the green areas and a polar group in the blue electrostatic potential areas (which were dominant close to the skeleton). As expected, the potent antifungal compounds (**5p**, **5w**) not only circumvented the red subregion or the unfavorable yellow steric subregion, but also got more close to the favorable blue and green spaces. Thus, this promising model would provide a guideline to design and optimize more effective derivatives against *R. solani* and pave the way for us in the further study.

Table 2 Experimental, predicted inhibitory activity of 1,2,3-triazole derivatives against human *R. solani* by 3D-QSAR models

Compound	Inhibition		Residual error
	Actual pEC ₅₀ ^b	Predicted pEC ₅₀	
5a	4.94	4.44	0.50
5b	5.34	4.87	0.47
5c	3.60	4.17	-0.57
5d	3.78	3.98	-0.20
5e^a	4.67	4.52	0.15
5f	5.28	5.36	-0.08
5g	5.26	5.11	0.15
5h^a	5.24	5.13	0.11
5i	4.83	4.41	0.42
5j^a	5.17	5.05	0.12
5k	3.78	4.10	-0.32
5l	5.03	5.00	0.03
5m^a	4.96	5.21	-0.25
5n	5.25	5.62	-0.37
5o^a	5.34	5.01	0.33
5p	6.24	5.54	0.70
5q	5.67	5.67	0.00
5r	6.07	5.79	0.28
5s	4.02	4.33	-0.31
5t	5.21	5.58	-0.37
5u	5.97	5.92	0.05
5v	5.44	5.27	0.17
5w	5.68	5.87	-0.19
5x	5.65	5.87	-0.22
5y	4.97	4.77	0.20
5z	5.31	5.69	-0.38

^a Compounds were selected as the test sets while the rest ones were in the training sets.

^b The EC₅₀ values of the compounds against TS were converted into pEC₅₀ values by using the online calculator. (<http://www.sanjeevlab.org/tools-IC50.html>).

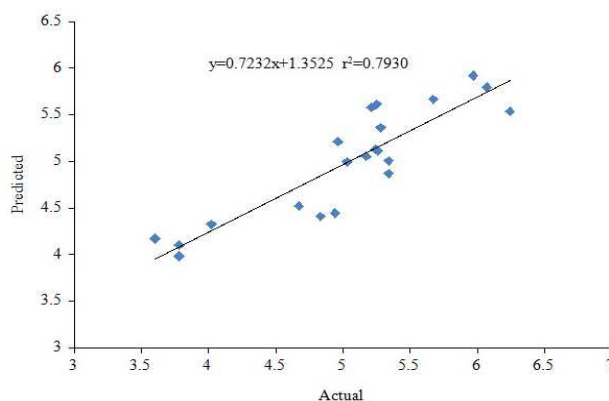


Figure 2. (A) The predicted versus experimental pEC₅₀ for *R. solani*.

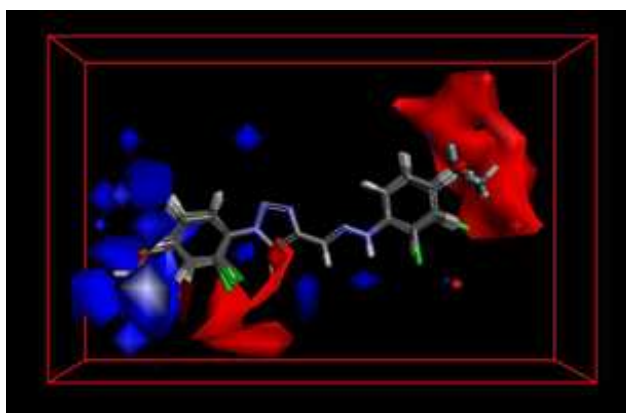


Figure 2. (B) Isosurface of the 3D-QSAR model coefficients on electrostatic potential grids.

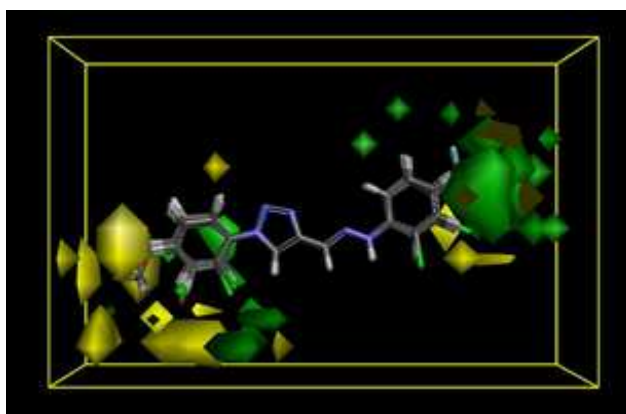


Figure 2. (C) Isosurface of the 3D-QSAR model coefficients on Van der Waals grids.

30 Protective activity of **5p** against RSB

Among the antifungal test *in vitro*, **5p** was regarded as the most potent one against *R. solani*. Therefore, it was selected and evaluated the protective activity against RSB caused by *R. solani* in the greenhouse. As shown in Figure 3 and Table 3, seven days after inoculating with *R. solani*, brown spots could be observed on the rice sheath of negative control, with the lesion length reached 17.2 mm. While at a concentration of 200 μg·mL⁻¹, the *in vivo* protective effect of **5p** could reach 91.8%, comparable to Validamycin A (91.2%), which is a commonly used fungicide

against RSB. When the concentration down to $100\mu\text{g}\cdot\text{mL}^{-1}$, **5p** was still effective against RSB (90.1%), which was significantly higher than that of Validamycin A (50.0%).

Protective activity of **5p** against RSR

As shown in Figure 4 and Table 4, compound **5p** not only significantly inhibited the mycelia growth of *S. sclerotiorum* *in vitro*, but also successfully suppressed disease development in *S. sclerotiorum* infected cole *in vivo*. The untreated negative control resulted in 100% RSR disease incidence (0% healthy plant standard) 36 h after transplantation. Treatment with 250 and 100 $\mu\text{g}\cdot\text{mL}^{-1}$ of **5p** resulted in 65.4% and 49.2% healthy plant standard, respectively, after 36 h of treatment. Although it was less effective than Carbendazim at the same concentrations

(84.1% and 79.4%), there are significant differences existed among the treated and untreated groups for RSR disease control experiments in the greenhouse cole leaves.

Protection efficacy against FHB of **5p** and **5w**

The efficacy of the protective activity experiment is shown in Table 5, two weeks after the inoculating of *F. graminearum*. The untreated negative control resulted in 100% FHB disease incidence, while **5p**, **5w** and Carbendazim resulted in 74.6%, 54.0%, 98.1%, respectively, when treated with $250\mu\text{g}\cdot\text{mL}^{-1}$. *In vivo* test demonstrated **5w** was better than **5p**, this could be caused by the difference in the wheat absorption of the two compounds. (Figure 5)



Fig 3. Protective activity of **5p** against RSB

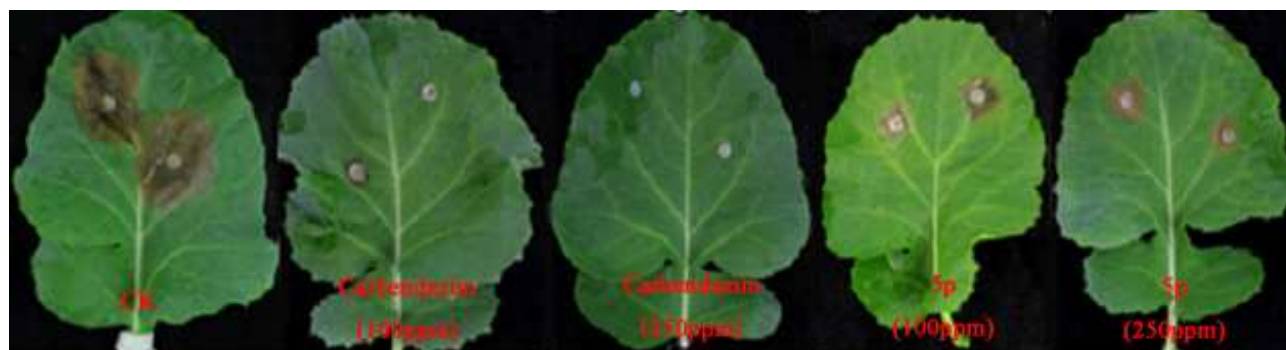


Fig 4. Protective activity of **5p** against RSR



Fig 5. Protection efficacy against FHB of **5p** and **5w**

Table 3 Protective activity of **5p** against RSB

	Treatment ($\mu\text{g}\cdot\text{mL}^{-1}$)	Lesion length ^a (mm)	Protection efficacy (%)
5p	200	1.4 ± 0.3	91.8
	100	1.7 ± 0.2	90.1
Validamycin A	200	1.5 ± 0.2	91.2
	100	8.6 ± 1.0	50.0
Negative control		17.2 ± 1.5	-

^aValues are the average of 20 replicates.**Table 4** Protective activity of **5p** against RSR

	Treatment ($\mu\text{g}\cdot\text{mL}^{-1}$)	Diameter of lesions ^a (mm)	Protection efficacy (%)
5p	250	10.9 ± 0.9	65.4
	100	16.0 ± 1.3	49.2
Carbendazim	250	5.0 ± 0.5	84.1
	100	6.5 ± 0.6	79.4
Negative control		31.5 ± 1.7	-

^aValues are the average of 10 replicates.**Table 5** Protection efficacy against FHB of **5p** and **5w**

	Treatment ($\mu\text{g}\cdot\text{mL}^{-1}$)	Disease index ^a	Protection efficacy (%)
5p	250	17.3	74.6
	50	49.7	26.9
5w	250	31.3	54.0
	50	51.7	24.0
Carbendazim	250	1.3	98.1
	50	23.0	66.2
Negative control		68.0	-

^aValues are the average of 30 replicates.

Experimental section

10 Chemistry

All reagents and solvents were of reagent grade or purified according to standard methods. Reactions were monitored by TLC using silica gel coated glass slides (silica gel 60 GF 254, Qingdao Haiyang Chemical, China). Detections were done in UV (254nm). Melting points were measured on a WRS-1B digital melting-point apparatus (SPSIC Shanghai, China); uncorrected. ¹H-NMR spectra were recorded on a Bruker Avance III 400 NMR spectrometer. The chemical shifts (δ) are reported in ppm with reference to internal TMS, and coupling constants (J) are given in Hz. HR-ESI-MS spectra were recorded on a Bruker UHR-TOF maxis mass spectrometer. X-ray single crystal diffraction analysis was conducted on a Bruker D8 Venture

diffractometer. Elemental analyses were determined on a CHN-O-Rapid instrument. The absorbances (ODs) were recorded on a SpectraMax M5 microplate reader (USA).

General Procedure for Preparation of 2a-k

In a round-bottom flask equipped with a magnetic stirring bar, substituted aniline (10 mmol) was dissolved with HCl (6N 10 mL) in ice bath. 25 mL water dissolved NaNO₂ (15 mmol) was added dropwise. The reaction mixture was stirred for 30 min. 50 mL water dissolved sodium azide (40 mmol) was added dropwise. After addition, the system was stirred for another 2-4 hours at room temperature. Then, the mixture was extracted with ethyl acetate and the combined organic extracts were washed with H₂O, dried over anhydrous Na₂SO₄, filtered, and concentrated *in vacuo*. The residual crude product was used directly without purification.

General Procedure for Preparation of 3a-k

In a round-bottom flask equipped with a magnetic stirring bar, sodium azide (1 mmol) was added, along with propargyl alcohol (1 mmol), CuSO₄ pentahydrate (0.05 mmol), sodium ascorbate (0.1 mmol), tert-butanol (7 mL), and H₂O (7 mL). The reaction mixture was stirred for 48-72 h at room temperature and subsequently extracted with ethyl acetate. The combined organic extracts were washed with H₂O, dried over anhydrous Na₂SO₄, filtered, and concentrated *in vacuo*. The residual crude product was purified via silica gel column chromatography using a gradient mixture of petroleum ether and ethyl acetate to obtain the pure derivatives **3a-k**.

General Procedure for Preparation of 4a-k

In a round-bottom flask equipped with a magnetic stirring bar, MnO₂ (150 mmol) and 10 mmol of 1,2,3-triazole **3a-k** were added to ethyl acetate (30 mL), the mixture was heated under reflux until **3a-k** fully consumed by the monitoring of thin layer chromatography (TLC). Afterwards the solution was filtered, and concentrated *in vacuo* to give pure aldehydes.

General Procedure for Preparation of 5a-z

The procedures were performed according to literature.¹⁹ Both equimolar aldehyde and substituted phenylhydrazine were mixed in MeOH and stirred in room temperature. After about 30 min, massive crystal particles were generated and separated out of the solution. Filtrations and recrystallizations (from MeOH / CH₂Cl₂) were performed to obtain **5a-z**. Except **5a** and **5d**, which were first prepared as glycosidase inhibitors using similar method by Gonzaga *et al.*,⁵ the other twenty-four compounds were novel.

(*E*)-1-phenyl-4-((2-phenylhydrazono)methyl)-1H-1,2,3-triazole (**5a**). Yellow powder, yield 70%. m.p. 163.9-164.1 °C. ¹H-NMR (400 MHz, DMSO-*d*₆) δ : 10.48 (s, 1H), 9.09 (s, 1H), 8.02 – 7.96 (m, 3H), 7.65 – 7.59 (m, 2H), 7.51 (t, J = 7.4 Hz, 1H), 7.26 – 7.21 (m, 2H), 7.09 (d, J = 7.6 Hz, 2H), 6.77 (t, J = 7.3 Hz, 1H). HRMS calcd for C₁₅H₁₄N₅ ([M+H]⁺): 264.1249; found: 264.1242. Anal. calcd. for C₁₅H₁₃N₅: C, 68.42; H, 4.98; N, 26.60. Found: C, 68.25; H, 4.76; N, 26.90.

(*E*)-1-(2-chlorophenyl)-4-((2-phenylhydrazono)methyl)-1H-1,2,3-triazole (**5b**). Light yellow powder, yield 75 %. m.p. 147.1-147.4 °C. ¹H-NMR (400 MHz, DMSO-*d*₆) δ : 11.28 (s, 1H), 8.96 (s, 1H), 7.89 – 7.77 (m, 2H), 7.74 – 7.60 (m, 2H), 7.36 (s, 1H), 7.28 (t, J = 7.8 Hz, 2H), 7.21 (d, J = 7.6 Hz, 2H), 6.86 (t, J = 7.2 Hz, 1H). HRMS calcd for C₁₅H₁₃ClN₅ ([M+H]⁺): 298.0859; found: 298.0848. Anal. calcd. for C₁₅H₁₂ClN₅: C, 60.51; H, 4.06; Cl, 11.91; N, 23.52. Found: C, 60.72; H, 4.16; Cl, 11.73; N, 23.48.

(*E*)-1-(3-chlorophenyl)-4-((2-phenylhydrazono)methyl)-1*H*-1,2,3-triazol (**5c**). White powder, yield 79 %. m.p. 168.7-168.8 °C. ¹H-NMR (400 MHz, DMSO-*d*₆) δ: 11.19 (s, 1H), 9.24 (s, 1H), 8.13 (s, 1H), 7.99 (d, *J* = 7.5 Hz, 1H), 7.77 – 7.56 (m, 2H), 7.41 – 7.13 (m, 5H), 6.86 (t, *J* = 7.0 Hz, 1H). HRMS calcd for C₁₅H₁₃ClN₅ ([M+H]⁺): 298.0859; found: 298.0858. Anal. calcd. for C₁₅H₁₂ClN₅: C, 60.51; H, 4.06; Cl, 11.91; N, 23.52. Found: C, 60.66; H, 4.09; Cl, 11.72; N, 23.44.

(*E*)-1-(4-chlorophenyl)-4-((2-phenylhydrazono)methyl)-1*H*-1,2,3-triazole (**5d**). Light yellow powder, yield 83 %. m.p. 196.6-197.3 °C. ¹H-NMR (400 MHz, DMSO-*d*₆) δ: 10.51 (s, 1H), 9.13 (s, 1H), 8.05 (d, *J* = 8.8 Hz, 2H), 8.00 (s, 1H), 7.70 (d, *J* = 8.8 Hz, 2H), 7.26 – 7.20 (m, 2H), 7.09 (d, *J* = 8.0 Hz, 2H), 6.78 (t, *J* = 7.2 Hz, 1H). HRMS calcd for C₁₅H₁₃ClN₅ ([M+H]⁺): 298.0859; found: 298.0852. Anal. calcd. for C₁₅H₁₂ClN₅: C, 60.51; H, 4.06; Cl, 11.91; N, 23.52. Found: C, 60.61; H, 4.08; Cl, 11.82; N, 23.56.

(*E*)-1-(2-bromophenyl)-4-((2-phenylhydrazono)methyl)-1*H*-1,2,3-triazole (**5e**). Yellow crystal, yield 68 %. m.p. 142.7-142.9 °C. ¹H-NMR (400 MHz, DMSO-*d*₆) δ: 11.30 (s, 1H), 8.95 (s, 1H), 7.97 (dd, *J* = 7.9, 1.2 Hz, 1H), 7.77 (dd, *J* = 7.7, 1.6 Hz, 1H), 7.68 (td, *J* = 7.6, 1.4 Hz, 1H), 7.62 (td, *J* = 7.8, 1.7 Hz, 1H), 7.36 (s, 1H), 7.28 (t, *J* = 7.8 Hz, 2H), 7.21 (d, *J* = 7.6 Hz, 2H), 6.86 (t, *J* = 7.2 Hz, 1H). HRMS calcd for C₁₅H₁₃BrN₅ ([M+H]⁺): 342.0354; found: 342.0343. Anal. calcd. for C₁₅H₁₂BrN₅: C, 52.65; H, 3.53; Br, 23.35; N, 20.47. Found: C, 52.45; H, 3.64; Br, 23.43; N, 20.46.

(*E*)-1-(3-bromophenyl)-4-((2-phenylhydrazono)methyl)-1*H*-1,2,3-triazole (**5f**). Light yellow powder, yield 70 %. m.p. 147.0-148.2 °C. ¹H-NMR (400 MHz, DMSO-*d*₆) δ: 10.52 (s, 1H), 9.20 (s, 1H), 8.27 (d, *J* = 11.3 Hz, 2H), 7.72 (d, *J* = 8.1 Hz, 1H), 7.58 (t, *J* = 8.1 Hz, 1H), 7.33 (s, 1H), 7.23 (d, *J* = 7.2 Hz, 2H), 7.09 (d, *J* = 7.8 Hz, 2H), 6.78 (t, *J* = 7.3 Hz, 1H). HRMS calcd for C₁₅H₁₃BrN₅ ([M+H]⁺): 342.0354; found: 342.0345. Anal. calcd. for C₁₅H₁₂BrN₅: C, 52.65; H, 3.53; Br, 23.35; N, 20.47. Found: C, 52.72; H, 3.49; Br, 23.25; N, 20.38.

(*E*)-1-(4-bromophenyl)-4-((2-phenylhydrazono)methyl)-1*H*-1,2,3-triazole (**5g**). Light yellow powder, yield 85 %. m.p. 201.1-201.3 °C. ¹H-NMR (400 MHz, DMSO-*d*₆) δ: 10.51 (s, 1H), 9.14 (s, 1H), 8.00 (s, 1H), 7.96 (d, *J* = 10.7 Hz, 2H), 7.83 (d, *J* = 8.8 Hz, 2H), 7.26 – 7.21 (m, 2H), 7.08 (d, *J* = 7.9 Hz, 2H), 6.78 (t, *J* = 7.3 Hz, 1H). HRMS calcd for C₁₅H₁₃BrN₅ ([M+H]⁺): 342.0354; found: 342.0344. Anal. calcd. for C₁₅H₁₂BrN₅: C, 52.65; H, 3.53; Br, 23.35; N, 20.47. Found: C, 52.80; H, 3.55; Br, 23.19; N, 20.36.

(*E*)-1-(2-fluorophenyl)-4-((2-phenylhydrazono)methyl)-1*H*-1,2,3-triazole (**5h**). White powder, yield 70 %. m.p. 132.8-133.2 °C. ¹H-NMR (400 MHz, DMSO-*d*₆) δ: 11.27 (s, 1H), 9.00 (d, *J* = 1.8 Hz, 1H), 7.94 (td, *J* = 7.9, 1.4 Hz, 1H), 7.73 – 7.60 (m, 2H), 7.55 – 7.47 (m, 1H), 7.37 (s, 1H), 7.28 (t, *J* = 7.8 Hz, 2H), 7.21 (d, *J* = 7.6 Hz, 2H), 6.86 (t, *J* = 7.2 Hz, 1H). HRMS calcd for C₁₅H₁₃FN₅ ([M+H]⁺): 282.1155; found: 282.1153. Anal. calcd. for C₁₅H₁₂FN₅: C, 64.05; H, 4.30; F, 6.75; N, 24.90. Found: C, 64.26; H, 4.22; F, 6.61; N, 24.75.

(*E*)-1-(3-fluorophenyl)-4-((2-phenylhydrazono)methyl)-1*H*-1,2,3-triazole (**5i**). White powder, yield 75 %. m.p. 155.5-155.6 °C. ¹H-NMR (400 MHz, DMSO-*d*₆) δ: 11.22 (s, 1H), 9.23 (s, 1H), 7.98 – 7.91 (m, 1H), 7.91 – 7.86 (m, 1H), 7.72 (dd, *J* = 14.5, 8.3 Hz, 1H), 7.44 (td, *J* = 8.5, 2.3 Hz, 1H), 7.34 (s, 1H), 7.32 –

7.26 (m, 2H), 7.21 (d, *J* = 7.6 Hz, 2H), 6.86 (t, *J* = 7.2 Hz, 1H). HRMS calcd for C₁₅H₁₃FN₅ ([M+H]⁺): 282.1155; found: 282.1151. Anal. calcd. for C₁₅H₁₂FN₅: C, 64.05; H, 4.30; F, 6.75; N, 24.90. Found: C, 64.35; H, 4.31; F, 6.62; N, 24.55.

(*E*)-1-(4-fluorophenyl)-4-((2-phenylhydrazono)methyl)-1*H*-1,2,3-triazol (**5j**). White powder, yield 83 %. m.p. 181.8-183.3 °C. ¹H-NMR (400 MHz, DMSO-*d*₆) δ: 11.26 (s, 1H), 9.15 (s, 1H), 8.08 – 8.01 (m, 2H), 7.53 (t, *J* = 8.8 Hz, 2H), 7.33 (s, 1H), 7.22 (dd, *J* = 15.3, 7.8 Hz, 3H), 7.08 (d, *J* = 7.7 Hz, 1H), 6.86 (t, *J* = 7.2 Hz, 1H). HRMS calcd for C₁₅H₁₃FN₅ ([M+H]⁺): 282.1155; found: 282.1148. Anal. calcd. for C₁₅H₁₂FN₅: C, 64.05; H, 4.30; F, 6.75; N, 24.90. Found: C, 64.26; H, 4.33; F, 6.71; N, 24.70.

(*E*)-1-(4-methoxyphenyl)-4-((2-phenylhydrazono)methyl)-1*H*-1,2,3-triazole (**5k**). White powder, yield 72 %. m.p. 166.1-170.0 °C. ¹H-NMR (400 MHz, DMSO-*d*₆) δ: 11.32 (s, 1H), 9.08 (s, 1H), 7.89 (d, *J* = 9.0 Hz, 2H), 7.32 (s, 1H), 7.31 – 7.26 (m, 2H), 7.20 (d, *J* = 9.0 Hz, 4H), 6.86 (t, *J* = 7.2 Hz, 1H), 3.86 (s, 3H). HRMS calcd for C₁₆H₁₆N₅O ([M+H]⁺): 294.1355; found: 294.1344. Anal. calcd. for C₁₆H₁₅N₅O: C, 65.52; H, 5.15; N, 23.88; O, 5.45. Found: C, 65.33; H, 5.17; N, 23.98; O, 5.55.

(*E*)-1-(2-chlorophenyl)-4-((2-(2-chlorophenyl)hydrazono)methyl)-1*H*-1,2,3-triazole (**5l**). Yellow crystal, yield 70 %. m.p. 97.7-97.9 °C. ¹H-NMR (400 MHz, DMSO-*d*₆) δ: 10.13 (s, 1H), 8.92 (s, 1H), 8.49 (s, 1H), 7.81 (dd, *J* = 7.9, 1.3 Hz, 1H), 7.76 (dd, *J* = 7.6, 1.8 Hz, 1H), 7.64 (dtd, *J* = 20.5, 7.5, 1.6 Hz, 2H), 7.56 (dd, *J* = 8.2, 1.2 Hz, 1H), 7.35 (dd, *J* = 7.9, 1.1 Hz, 1H), 7.25 (t, *J* = 7.7 Hz, 1H), 6.81 (td, *J* = 7.8, 1.4 Hz, 1H). HRMS calcd for C₁₅H₁₂Cl₂N₅ ([M+H]⁺): 332.0470; found: 332.0468. Anal. calcd. for C₁₅H₁₁Cl₂N₅: C, 54.23; H, 3.34; Cl, 21.35; N, 21.08. Found: C, 54.35; H, 3.31; Cl, 21.27; N, 21.04.

(*E*)-1-(2-chlorophenyl)-4-((2-(3-chlorophenyl)hydrazono)methyl)-1*H*-1,2,3-triazole (**5m**). White powder, yield 75 %. m.p. 147.3-148.3 °C. ¹H-NMR (400 MHz, DMSO-*d*₆) δ: 11.28 (s, 1H), 9.01 (s, 1H), 7.84 (dd, *J* = 8.0, 1.2 Hz, 1H), 7.81 (dd, *J* = 7.7, 1.5 Hz, 1H), 7.71 (td, *J* = 7.8, 1.8 Hz, 1H), 7.65 (td, *J* = 7.6, 1.4 Hz, 1H), 7.44 (s, 1H), 7.33 – 7.25 (m, 2H), 7.16 (dd, *J* = 8.0, 1.5 Hz, 1H), 6.89 (d, 1H). HRMS calcd for C₁₅H₁₂Cl₂N₅ ([M+H]⁺): 332.0470; found: 332.0462. Anal. calcd. for C₁₅H₁₁Cl₂N₅: C, 54.23; H, 3.34; Cl, 21.35; N, 21.08. Found: C, 54.44; H, 3.28; Cl, 21.36; N, 21.12.

(*E*)-1-(2-chlorophenyl)-4-((2-(4-chlorophenyl)hydrazono)methyl)-1*H*-1,2,3-triazole (**5n**). Yellow powder, yield 78 %. m.p. 105.9-106.9 °C. ¹H-NMR (400 MHz, DMSO-*d*₆) δ: 10.62 (s, 1H), 8.85 (s, 1H), 8.03 (s, 1H), 7.80 (dd, *J* = 7.9, 1.3 Hz, 1H), 7.75 (dd, *J* = 7.7, 1.7 Hz, 1H), 7.69 – 7.58 (m, 2H), 7.26 (d, *J* = 8.8 Hz, 2H), 7.05 (d, *J* = 8.8 Hz, 2H). HRMS calcd for C₁₅H₁₂Cl₂N₅ ([M+H]⁺): 332.0470; found: 332.0464. Anal. calcd. for C₁₅H₁₁Cl₂N₅: C, 54.23; H, 3.34; Cl, 21.35; N, 21.08. Found: C, 54.34; H, 3.38; Cl, 21.46; N, 21.22.

(*E*)-1-(2-chlorophenyl)-4-((2-(2-fluorophenyl)hydrazono)methyl)-1*H*-1,2,3-triazole (**5o**). Yellow crystal, yield 68 %. m.p. 150.1-150.9 °C. ¹H-NMR (400 MHz, DMSO-*d*₆) δ: 1H NMR (400 MHz, DMSO) δ 10.44 (s, 1H), 8.89 (s, 1H), 8.31 (s, 1H), 7.81 (dd, *J* = 7.8, 1.0 Hz, 1H), 7.76 (dd, *J* = 7.6, 1.7 Hz, 1H), 7.70 – 7.60 (m, 2H), 7.50 (t, *J* = 8.3 Hz, 1H), 7.19 – 7.12 (m, 1H), 7.09 (t, *J* = 7.7 Hz, 1H), 6.77 (ddd, *J* = 9.0, 7.6, 1.3 Hz, 1H). HRMS calcd for C₁₅H₁₂ClFN₅ ([M+H]⁺): 316.0765; found: 316.0758. Anal. calcd. for C₁₅H₁₁ClFN₅: C, 57.06; H, 3.51; Cl, 11.23; F,

6.02; N, 22.18. Found: C, 57.28; H, 3.41; Cl, 11.33; F, 6.03; N, 22.07.

(*E*)-1-(2-chlorophenyl)-4-((2-(4-fluorophenyl)hydrazono)methyl)-1*H*-1,2,3-triazole (**5p**). Brown crystal, yield 73 %. m.p. 100.7-100.8 °C. ¹H-NMR (400 MHz, DMSO-*d*₆) δ: 10.47 (s, 1H), 8.82 (s, 1H), 8.01 (s, 1H), 7.80 (dd, *J* = 7.9, 1.4 Hz, 1H), 7.75 (dd, *J* = 7.6, 1.8 Hz, 1H), 7.66 (td, *J* = 7.7, 1.9 Hz, 1H), 7.61 (td, *J* = 7.6, 1.5 Hz, 1H), 7.10 – 7.01 (m, 4H). HRMS calcd for C₁₅H₁₂ClFN₅ ([M+H]⁺): 316.0765; found: 316.0758. Anal. calcd. for C₁₅H₁₁ClFN₅: C, 57.06; H, 3.51; Cl, 11.23; F, 6.02; N, 22.18. Found: C, 57.35; H, 3.44; Cl, 11.20; F, 6.05; N, 22.05.

(*E*)-4-((2-(4-bromophenyl)hydrazono)methyl)-1-(2-chlorophenyl)-1*H*-1,2,3-triazole (**5q**). Light yellow powder, yield 83 %. m.p. 133.2-134.4 °C. ¹H-NMR (400 MHz, DMSO-*d*₆) δ: 10.63 (s, 1H), 8.85 (s, 1H), 8.03 (s, 1H), 7.80 (dd, *J* = 7.9, 1.5 Hz, 1H), 7.75 (dd, *J* = 7.6, 1.8 Hz, 1H), 7.66 (td, *J* = 7.7, 1.9 Hz, 1H), 7.61 (td, *J* = 7.6, 1.5 Hz, 1H), 7.37 (d, *J* = 8.9 Hz, 2H), 7.01 (d, *J* = 8.9 Hz, 2H). HRMS calcd for C₁₅H₁₂BrClN₅ ([M+H]⁺): 375.9965; found: 375.9963. Anal. calcd. for C₁₅H₁₁BrClN₅: C, 47.83; H, 2.94; Br, 21.22; Cl, 9.41; N, 18.59. Found: C, 47.66; H, 2.87; Br, 21.45; Cl, 9.38; N, 18.63.

(*E*)-1-(2-chlorophenyl)-4-((2-(4-(trifluoromethyl)phenyl)hydrazono)methyl)-1*H*-1,2,3-triazole (**5r**). Red crystal, yield 79 %. m.p. 152.5-153.4 °C. ¹H-NMR (400 MHz, DMSO-*d*₆) δ: 10.94 (s, 1H), 8.91 (s, 1H), 8.11 (s, 1H), 7.81 (dd, *J* = 7.9, 1.4 Hz, 1H), 7.76 (dd, *J* = 7.7, 1.7 Hz, 1H), 7.67 (td, *J* = 7.8, 1.8 Hz, 1H), 7.61 (td, *J* = 7.6, 1.5 Hz, 1H), 7.55 (d, *J* = 8.7 Hz, 2H), 7.18 (d, *J* = 8.5 Hz, 2H). HRMS calcd for C₁₆H₁₂ClF₃N₅ ([M+H]⁺): 366.0733; found: 366.0732. Anal. calcd. for C₁₆H₁₁ClF₃N₅: C, 52.54; H, 3.03; Cl, 9.69; F, 15.58; N, 19.15. Found: C, 52.74; H, 3.28; Cl, 9.63; F, 15.44; N, 19.03.

(*E*)-4-((2-(2-chlorophenyl)hydrazono)methyl)-1-(2-fluorophenyl)-1*H*-1,2,3-triazole (**5s**). White powder, yield 77 %. m.p. 135.4-135.9 °C. ¹H-NMR (400 MHz, DMSO-*d*₆) δ: 10.15 (s, 1H), 8.95 (d, *J* = 1.9 Hz, 1H), 8.48 (s, 1H), 7.90 (td, *J* = 7.8, 1.5 Hz, 1H), 7.66 – 7.60 (m, 2H), 7.58 (dd, *J* = 8.2, 1.2 Hz, 1H), 7.50 – 7.44 (m, 1H), 7.35 (dd, *J* = 7.9, 1.3 Hz, 1H), 7.29 – 7.22 (m, 1H), 6.82 (td, *J* = 7.7, 1.5 Hz, 1H). HRMS calcd for C₁₅H₁₂ClFN₅ ([M+H]⁺): 316.0765; found: 316.0761. Anal. calcd. for C₁₅H₁₁ClFN₅: C, 57.06; H, 3.51; Cl, 11.23; F, 6.02; N, 22.18. Found: C, 57.29; H, 3.48; Cl, 11.30; F, 6.06; N, 22.03.

(*E*)-4-((2-(3-chlorophenyl)hydrazono)methyl)-1-(2-fluorophenyl)-1*H*-1,2,3-triazole (**5t**). Yellow powder, yield 74 %. m.p. 137.2-138.1 °C. ¹H-NMR (400 MHz, DMSO-*d*₆) δ: 10.72 (s, 1H), 8.95 (d, *J* = 1.8 Hz, 1H), 8.05 (s, 1H), 7.89 (td, *J* = 7.9, 1.5 Hz, 1H), 7.68 – 7.56 (m, 2H), 7.49 – 7.43 (m, 1H), 7.24 (t, *J* = 8.0 Hz, 1H), 7.15 (t, *J* = 2.0 Hz, 1H), 6.94 (dd, *J* = 8.2, 1.3 Hz, 1H), 6.79 (dd, 1H). HRMS calcd for C₁₅H₁₂ClFN₅ ([M+H]⁺): 316.0765; found: 316.0768. Anal. calcd. for C₁₅H₁₁ClFN₅: C, 57.06; H, 3.51; Cl, 11.23; F, 6.02; N, 22.18. Found: C, 57.34; H, 3.45; Cl, 11.19; F, 6.12; N, 22.12.

(*E*)-4-((2-(4-chlorophenyl)hydrazono)methyl)-1-(2-fluorophenyl)-1*H*-1,2,3-triazole (**5u**). White powder, yield 83 %. m.p. 148.2-149.1 °C. ¹H-NMR (400 MHz, DMSO-*d*₆) δ: 10.63 (s, 1H), 8.87 (d, *J* = 1.8 Hz, 1H), 8.03 (s, 1H), 7.89 (td, *J* = 7.9, 1.3 Hz, 1H), 7.69 – 7.56 (m, 2H), 7.46 (dd, *J* = 11.6, 4.8 Hz, 1H), 7.26 (d, *J* = 8.8 Hz, 2H), 7.07 (d, *J* = 8.8 Hz, 2H). HRMS calcd for C₁₅H₁₂ClFN₅ ([M+H]⁺): 316.0765; found: 316.0761. Anal. calcd.

for C₁₅H₁₁ClFN₅: C, 57.06; H, 3.51; Cl, 11.23; F, 6.02; N, 22.18. Found: C, 57.24; H, 3.49; Cl, 11.16; F, 6.09; N, 22.05.

(*E*)-1-(2-fluorophenyl)-4-((2-(2-fluorophenyl)hydrazono)methyl)-1*H*-1,2,3-triazole (**5v**). Light yellow powder, yield 68 %. m.p. 115.4-116.9 °C. ¹H-NMR (400 MHz, DMSO-*d*₆) δ: 10.46 (s, 1H), 8.92 (d, *J* = 1.9 Hz, 1H), 8.31 (s, 1H), 7.90 (td, *J* = 7.9, 1.5 Hz, 1H), 7.63 (ddd, *J* = 10.3, 5.3, 3.5 Hz, 2H), 7.53 – 7.45 (m, 2H), 7.21 – 7.15 (m, 1H), 7.11 (t, *J* = 7.7 Hz, 1H), 6.83 – 6.75 (m, 1H). HRMS calcd for C₁₅H₁₂F₂N₅ ([M+H]⁺): 300.1061; found: 300.1064. Anal. calcd. for C₁₅H₁₁F₂N₅: C, 60.20; H, 3.70; F, 12.70; N, 23.40. Found: C, 60.43; H, 3.65; F, 12.64; N, 23.30.

(*E*)-1-(2-fluorophenyl)-4-((2-(4-fluorophenyl)hydrazono)methyl)-1*H*-1,2,3-triazole (**5w**). Light yellow powder, yield 70 %. m.p. 115.1-115.8 °C. ¹H-NMR (400 MHz, DMSO-*d*₆) δ: 10.49 (s, 1H), 8.85 (d, *J* = 1.9 Hz, 1H), 8.01 (s, 1H), 7.89 (td, *J* = 7.9, 1.5 Hz, 1H), 7.69 – 7.56 (m, 2H), 7.51 – 7.42 (m, 1H), 7.12 – 7.02 (m, 4H). HRMS calcd for C₁₅H₁₂F₂N₅ ([M+H]⁺): 300.1061; found: 300.1060. Anal. calcd. for C₁₅H₁₁F₂N₅: C, 60.20; H, 3.70; F, 12.70; N, 23.40. Found: C, 60.32; H, 3.52; F, 12.55; N, 23.38.

(*E*)-4-((2-(4-bromophenyl)hydrazono)methyl)-1-(2-fluorophenyl)-1*H*-1,2,3-triazole (**5x**). Yellow powder, yield 73 %. m.p. 115.1-115.8 °C. ¹H-NMR (400 MHz, DMSO-*d*₆) δ: 10.64 (s, 1H), 8.87 (d, *J* = 1.9 Hz, 1H), 8.03 (s, 1H), 7.89 (td, *J* = 7.9, 1.4 Hz, 1H), 7.69 – 7.56 (m, 2H), 7.46 (dd, *J* = 11.7, 5.0 Hz, 1H), 7.38 (d, *J* = 8.8 Hz, 2H), 7.02 (d, *J* = 8.8 Hz, 2H). HRMS calcd for C₁₅H₁₂BrFN₅ ([M+H]⁺): 360.0260; found: 360.0258. Anal. calcd. for C₁₅H₁₁BrFN₅: C, 50.02; H, 3.08; Br, 22.18; F, 5.27; N, 19.44. Found: C, 50.33; H, 3.01; Br, 22.08; F, 5.14; N, 19.39.

(*E*)-1-(2-fluorophenyl)-4-((2-(4-methoxyphenyl)hydrazono)methyl)-1*H*-1,2,3-triazole (**5y**). Yellow powder, yield 75 %. m.p. 92.6-93.3 °C. ¹H-NMR (400 MHz, DMSO-*d*₆) δ: 10.30 (s, 1H), 8.80 (d, *J* = 1.9 Hz, 1H), 7.97 (s, 1H), 7.89 (td, *J* = 7.9, 1.5 Hz, 1H), 7.61 (dd, *J* = 21.1, 8.2 Hz, 2H), 7.53 – 7.43 (m, 1H), 7.01 (d, *J* = 8.9 Hz, 2H), 6.85 (d, *J* = 9.0 Hz, 2H), 3.70 (s, 3H). HRMS calcd for C₁₆H₁₅FN₅O ([M+H]⁺): 312.1261; found: 312.1256. Anal. calcd. for C₁₆H₁₄FN₅O: C, 61.73; H, 4.53; F, 6.10; N, 22.50; O, 5.14. Found: C, 61.84; H, 4.64; F, 6.05; N, 22.33; O, 5.07.

(*E*)-1-(2-fluorophenyl)-4-((2-(*p*-tolyl)hydrazono)methyl)-1*H*-1,2,3-triazole (**5z**). Yellow powder, yield 77 %. m.p. 110.8-111.7 °C. ¹H-NMR (400 MHz, DMSO-*d*₆) δ: 10.39 (s, 1H), 8.82 (s, 1H), 7.98 (s, 1H), 7.89 (td, *J* = 7.9, 1.5 Hz, 1H), 7.63 – 7.57 (m, 1H), 7.49 – 7.44 (m, 1H), 7.10 (d, *J* = 1.7 Hz, 1H), 7.04 (d, *J* = 8.3 Hz, 2H), 6.97 (d, *J* = 8.5 Hz, 2H), 2.21 (s, 3H). HRMS calcd for C₁₆H₁₅FN₅ ([M+H]⁺): 296.1311; found: 296.1310. Anal. calcd. for C₁₆H₁₄FN₅: C, 65.07; H, 4.78; F, 6.43; N, 23.71. Found: C, 65.21; H, 4.53; F, 6.33; N, 23.83.

Crystallographic study

X-ray single-crystal diffraction data for compound **5i** were collected on a Bruker SMART APEX CCD diffractometer at 273(2) K using Mo K α radiation ($\lambda=0.71073$ Å) by the π and ω scan mode. The program SAINT was used for integration of the diffraction profiles. Structure was solved by direct methods using the SHELXS program of the SHELXTL package and refined by full-matrix least-squares methods with SHELXL.²⁰ All non-hydrogen atoms of compound **5i** were refined with anisotropic thermal parameters. All hydrogen atoms were placed in geometrically idealized positions and constrained to ride on their

parent atoms.

Antifungal activity assay

The fungicidal activities were tested *in vitro* against four plant-pathogenic fungi (*R. solani*, *S. sclerotiorum*, *F. graminearum*, and *P. capsici*) using the mycelia growth inhibition method on PDA.²¹ Compounds were dissolved in DMSO to prepare 1.0×10^4 mg·mL⁻¹ stock solution before mixing with sterile molten PDA below 60°C. We choose 25 μg·mL⁻¹ as the initial screening concentration to identify which kind of the compounds were more potential. Compounds possessing good activities (inhibitory rate >50% at 25 μg·mL⁻¹) were further evaluated with different concentrations. After a certain incubation period (1.5 d for *R. solani*, 2.5 d for *S. sclerotiorum*, 3 d for *F. graminearum*, and 4 d for *P. capsici*) at 25 °C in dark, the colony diameter of each strain was measured. Percentage inhibition was calculated as $(B-A) / (B-5) \times 100 \%$, where A is the mycelial diameter (mm) in Petri dishes with compounds and B is the diameter (mm) of negative control. Three replicates were used per treatment. DMSO served as negative control, where as commercially available agricultural fungicide Validamycin A, Carbendazim and Metalaxyl were used as positive controls (Table 1).

3D-QSAR

Ligand-based 3D-QSAR approach was performed by QSAR module of DS 3.5 (Discovery Studio 3.5, Accelrys, Co. Ltd). The training sets were composed of 21 inhibitors with the corresponding pEC₅₀ values which were converted from the obtained EC₅₀ (μM), and test sets comprised 5 compounds of data sets as list in Table 2.

All the definition of the descriptors can be seen in the Help of DS3.5 software and they were calculated by QSAR protocol of DS3.5.34. We can believe that the modeling is reliable, when the r² for test sets is larger than 0.6, respectively.

Evaluation of protective activity of 5p against RSB

To evaluate the protective activity of **5p**, rice cultivar (Shanyou 63) was grown in plastic pots (diameter of 18 cm × height of 20 cm) in the greenhouse. The cultivar was planted following normal agronomic practices and infected by *R. solani* which was artificially inoculated by reported method.²² Validamycin A (5% AS, Wuhan Kenuo Biochemical Co., Ltd., China) as the positive control. Visual disease assessment was made 7 days after the inoculating of *R. solani* (different concentration of compounds were sprayed on plants 24 h before inoculation). And the protective control efficacies were calculated as follows: Protection efficacy = [(average lesion length of control – average lesion length of treated group) / average lesion length of control] × 100%. Disease severity = [(the number of diseased plants in this index × disease index) / (total number of plants investigated × the highest disease index)] × 100%. Control efficacy = [(disease severity of control – disease severity of treated group) / disease severity of control] × 100%.

Protective activity of 5p against RSR

Strain *S. sclerotiorum* and susceptible cole leaves collected from Pailou (Experimental Centre of Nanjing Agricultural University) were used to measure the efficacy of compounds *in vivo*. Healthy cole leaves were sprayed with compounds and subsequently

cultivated at 25°C for 24 h before artificial inoculation with strain *S. sclerotiorum*. Results were observed as diameters of symptoms after cultivation at 20°C for 36 h. Carbendazim (50% WP, Jiangsu Rotam Lanfeng Biochemical Co., Ltd., China) was co assayed as the positive control. The efficacy of disease control was calculated as $(1 - c/d) \times 100\%$, where *c* is the diameter of the treatment and *d* is the diameter of the negative control.²³

Protection efficacy against FHB of 5p and 5w

The strain *F. graminearum* and *F. graminearum*-susceptible wheat cultivar Yangmai 2 were used to evaluate the protective activity of **5p** and **5w** at greenhouse of Pailou. When anthesis approached, plants were sprayed with different treatments so that the solution was applied at 75 mL/m² by using a precision hand sprayer. One day later, wheat spikes were inoculated with the *F. graminearum* strain 2021. Inoculation was achieved by injecting the prepared conidial suspension into spikes using a pipette at a dosage of 10 μL per spike. Carbendazim (50% WP, Jiangsu Rotam Lanfeng Biochemical Co., Ltd., China) was co assayed as the positive control. Visual disease assessment was made 15 days after the inoculating of *F. graminearum*. And the protective control efficacy were calculated as follows: Protection efficacy = [(number of infected spikelet of control – number of infected spikelet of treated group) / number of infected spikelet of control] × 100%. Disease severity = [(number of infected spikelet in this index × disease index) / (total number of plants investigated × the highest disease index)] × 100%. Control efficacy = [(disease severity of control – disease severity of treated group) / disease severity of control] × 100%.²⁴

Conclusion

In conclusion, a series of 1,2,3-triazole phenylhydrazones were designed, synthesized and evaluated for their antifungal activity against four important phytopathogens, namely *R. solani*, *S. sclerotiorum*, *F. graminearum* and *P. capsici*. Most of them displayed considerable inhibitory activities against *R. solani*. 3D-QSAR model was built to obtain a systematic SAR profile on 1,2,3-triazole phenylhydrazones to explore the more potent inhibitors. The **5p** showed good activity against RSB with protective efficacy of 90.1 % at 100 μg·mL⁻¹, which was significantly higher than Validamycin A (50.0 %). At the same time, the protective activity of **5p** against RSR can reach 65.4 % at 250 μg·mL⁻¹, while positive control Carbendazim was 84.1 %. Although compound **5w** displayed the maximum antifungal activity against *F. graminearum* (EC₅₀ = 0.61 μg/mL⁻¹) *in vitro*, which is comparable with Carbendazim (EC₅₀ = 0.50 μg/mL⁻¹), the *in vivo* activity against FHB was still worse than **5p** (74.6 %). The broad-spectrum antifungal effects of the new 1,2,3-triazole phenylhydrazones qualified them as potential antifungal candidates and **5p** might be considered as a promising lead compound for further research.

Acknowledgements

This work was co-supported by National Basic Research Program of China (2010CB126100), Natural Science Foundation of Jiangsu Province (BK20140684). Fundamental Research Funds for the Central Universities (KYZ201107), and Special Fund for

Agro-scientific Research in the Public Interest (201303023).

Notes and references

^aCollege of Plant Protection, State & Local Joint Engineering Research Center of Green Pesticide Invention and Application, Nanjing

⁵Agricultural University, Nanjing 210095, P. R. China. Fax: +86-25-84399753; Tel: +86-25-84399753; E-mail: yeyh@njau.edu.cn,

^bKey Laboratory of Integrated Management of Crop Diseases and Pests, Ministry of Education, Nanjing 210095, P. R. China

^cMedical College, Yangzhou University, Yangzhou 225001, P. R. China.

¹⁰^dSchool of Life Sciences, Shandong University of Technology, Zibo 255049, People's Republic of China

^eDepartment of Medicinal Chemistry, School of Pharmacy, Fudan University, Shanghai 201203, People's Republic of China

- 15 1. R. A. Wilson, N. J. Talbot, *Microbiology* 2009, **155**, 3810.
2. V. Sumangala, B. Poojary, N. Chidananda, J. Fernandes, N. S. Kumari, *Arch. Pharm. Res.*, 2010, **33**, 1911.
3. K. Karthik Kumar, S. Prabu Seenivasan, V. Kumar, T. Mohan Das, *Carbohydr. Res.*, 2011, **346**, 2084.
- 20 4. F. C. da Silva, M. C. B. de Souza, I. I. Frugulhetti, H. C. Castro, S. L. d. O. Souza, T. M. L. de Souza, D. Q. Rodrigues, A. M. Souza, P. A. Abreu, F. Passamani, *Eur. J. Med. Chem.*, 2009, **44**, 373.
5. D. Gonzaga, M. R. Senger, C. da Silva Fde, V. F. Ferreira, F. P. Silva, Jr., *Eur. J. Med. Chem.*, 2014, **74**, 461.
- 25 6. Y. Qin, S. Liu, R. Xing, K. Li, H. Yu, P. Li, *Int. J. Biol. Macromol.*, 2013, **61**, 58.
7. M. Z. Mao, Y. X. Li, Y. Y. Zhou, W. Chen, T. W. Liu, S. J. Yu, S. H. Wang, Z. M. Li, *Chem. Biol. Drug. Des.* 2011, **78**, 695.
8. M. Gaur, M. Goel, L. Sridhar, T. D. S. Ashok, S. Prabhakar, P. Dureja, P. Raghunathan, S. V. Eswaran, *Monatsh. Chem.*, 2012, **143**, 283.
- 30 9. G. Klopman, D. Ptchelintsev, *J. Comput.-Aided Mol. Des.*, 1993, **7**, 349.
10. D. Mares, C. Romagnoli, E. Andreotti, M. Manfrini, C. B. Vicentini, *J. Agr. Food. Chem.*, 2004, **52**, 2003.
- 35 11. R. P. Tripathi, A. K. Yadav, A. Ajay, S. S. Bisht, V. Chaturvedi, S. K. Sinha, *Eur. J. Med. Chem.*, 2010, **45**, 142.
12. D. I. Rozkiewicz, D. Jańczewski, W. Verboom, B. J. Ravoo, D. N. Reinhoudt, *Angew. Chem. Int. Edit.*, 2006, **45**, 5292.
13. G. Zinzalla, D. E. Thurston, *Future Med. Chem.* 2009, **1**, 65.
- 40 14. D. M. Neumann, A. Cammarata, G. Backes, G. E. Palmer, B. S. Jursic, *Bioorgan. Med. Chem.*, 2014, **22**, 813.
15. N. Boechat, V. F. Ferreira, S. B. Ferreira, G. F. M. de Lourdes, C. d. S. F. de, M. M. Bastos, S. C. M. Dos, M. C. Lourenco, A. C. Pinto, A. U. Krettli, A. C. Aguiar, B. M. Teixeira, N. V. da Silva, P. R.
- 45 Martins, F. A. Bezerra, A. L. Camilo, G. P. da Silva, C. C. Costa, *J. Med. Chem.*, 2011, **54**, 5988.
16. M. S. Costa, N. Boechat, E. A. Rangel, C. da Silva Fde, A. M. de Souza, C. R. Rodrigues, H. C. Castro, I. N. Junior, M. C. Lourenco, S. M. Wardell, V. F. Ferreira, *Bioorgan. Med. Chem.*, 2006, **14**, 8644.
- 50 17. M. Chen, X. F. Wang, S. S. Wang, Y. X. Feng, F. Chen, C. L. Yang, *J. Fluorine Chem.* 2012, **135**, 323.
18. Q. R. Du, D. D. Li, Y. Z. Pi, J. R. Li, J. Sun, F. Fang, W. Q. Zhong, H. B. Gong, H. L. Zhu, *Bioorgan. Med. Chem.*, 2013, **21**, 2286.
- 55 19. N. Belkheiri, B. Bouguerne, F. Bedos-Belval, H. Duran, C. Bernis, R. Salvayre, A. Nègre-Salvayre, M. Baltas, *Eur. J. Med. Chem.*, 2010, **45**, 3019.
20. A. Altomare, G. Cascarano, C. Giacobuzzo, A. Guagliardi, M. Burla, G. t. Polidori, M. Camalli, *J. Appl. Crystallogr.*, 1994, **27**, 435.
- 60 21. Y. Xiao, H. X. Li, C. Li, J. X. Wang, J. Li, M. H. Wang, Y. H. Ye, *Fems. Microbiol. Lett.*, 2013, **339**, 130.
22. D. Peng, S. Li, J. Wang, C. Chen, M. Zhou, *Pest. Manag. Sci.*, 2014, **70**, 258.
23. L. L. Wang, C. Li, Y. Y. Zhang, C. H. Qiao, Y. H. Ye, *J. Agr. Food. Chem.*, 2013, **61**, 8632.
- 65 24. Y. Chen, M. G. Zhou, *Pest. Manag. Sci.*, 2009, **65**, 398.